



OPEN

Innovative textiles treated with TiO₂-AgNPs with succinic acid as a cross-linking agent for medical uses

Mohamed Abdel-Shakur Ali¹✉, Emam Abdel-Mobdy Abdel-Rahim¹, Azza Abdel-Aziz Mahmoud² & Sahar Emam Mohamed²

Silver and titanium-silver nanoparticles have unique properties that make the textile industry progress through the high quality of textiles. Preparation of AgNPs and TiO₂-Ag core-shell nanoparticles in different concentrations (0.01% and 0.1% OWF) and applying it to cotton fabrics (Giza 88 and Giza 94) by using succinic acid 5%/SHP as a cross-linking agent. Ultra-violet visible spectroscopy (UV-Vis), X-ray diffraction (XRD), dynamic light scattering (DLS), zeta potential, transmission electron microscopy (TEM), scanning electron microscopy/energy-dispersive X-ray (SEM-EDX) are tools for AgNPs and TiO₂-AgNPs characterization and the treated cotton. The resulting AgNPs and TiO₂-AgNPs were added to cotton fabrics at different concentrations. The antimicrobial activities, UV protection, self-cleaning, and the treated fabrics' mechanical characteristics were investigated. Silver nanoparticles and titanium dioxide-silver nanoparticles core-shell were prepared to be used in the treatment of cotton fabrics to improve their UV protection properties, self-cleaning, elongation and strength, as well as the antimicrobial activities to use the produced textiles for medical and laboratory uses and to increase protection for medical workers taking into account the spread of infection. The results demonstrated that a suitable distribution of prepared AgNPs supported the spherical form. Additionally, AgNPs and TiO₂-AgNPs have both achieved stability, with values of (–20.8 mV and –30 mV, respectively). The synthesized nanoparticles spread and penetrated textiles' surfaces with efficiency. The findings demonstrated the superior UV protection value (UPF 50+) and self-cleaning capabilities of AgNPs and TiO₂-AgNPs. In the treatment with 0.01% AgNPs and TiO₂-AgNPs, the tensile strength dropped, but the mechanical characteristics were enhanced by raising the concentration to 0.1%. The results of this investigation demonstrated that the cotton fabric treated with TiO₂-AgNPs exhibited superior general characteristics when compared to the sample treated only with AgNPs.

Keywords Silver nanoparticles, Titanium dioxide nanoparticles, Core-shell, UV protection, Self-cleaning, Antimicrobial, Textiles and cotton fabrics

Abbreviations

AgNPs	Silver nanoparticles
DLS	Dynamic light scattering
G88	Giza 88
G94	Giza 94
OWF	On the weight of fabric
PS	Particle size
SEM-EDX	Scanning electron microscopy/energy-dispersive X-ray
SHP	Sodium hypophosphate
TEM	Transmission electron microscopy
TiO ₂ -AgNPs	Titanium oxide-silver nanoparticles

¹Biochemistry Department, Faculty of Agriculture, Cairo University, Giza, Egypt. ²Cotton Technology Research Division, Cotton Research Institute, Agriculture Research Center, Giza, Egypt. ✉email: mohamed_soliman@cu.edu.eg

TUV	Transmitted ultraviolet
UPF	Ultraviolet protection factor
UV-Vis	Ultra-violet visible spectroscopy
XRD	X-ray diffraction
ZP	Zeta potential

Commercialization applications of nanoparticles, particularly self-cleaning and antibacterial technical textiles, offer enormous potential for the technical textile sector. By incorporating metal and metal oxide nanoparticles into textile finishing operations, such nano-based high-performance textiles may be created right away^{1,2}. Metallic NPs have tremendous potential that may be effectively used to create useful fabrics. Metallic-based particles can provide intriguing finishes without detracting from the fabrics' look or negatively affecting their properties. According to numerous studies^{3–5} textiles can be treated with silver, titanium dioxide, zinc oxide and silicon dioxide nanoparticles as surface-modifying agents to add various properties like ultraviolet protection, self-cleaning, and antimicrobial activities. The treated cotton fabric showed durable super hydrophobicity, dye degradation, and antibacterial activity with UPF more than 90 up to 20 industrial laundering cycles. The highest water contact angle obtained was 150.5° which was reduced to 131° after 20 washing cycles. The treated fabric exhibited good antibacterial activity against bacteria (*S. aureus* and *E. coli*) even after 20 industrial laundering cycles showing good durability of NPs without having any significant effect on physical properties of fabric after treatment (3–5). Recently, it has been reported that titanium dioxide nanoparticles may be adhered to fabric surfaces using a variety of techniques such as drop casting, dip coating, optical deposition, layer-by-layer deposition, electrospin and electrospraying to create a self-cleaning surface. Among these techniques, drop casting and dip coating are the simplest ones, whereas optical deposition allows monitoring the process of coating, layer-by-layer deposition is time-consuming technique, and electrospin/electrospraying technique required special equipment⁶.

It has been demonstrated that titanium dioxide nanoparticles have photocatalytic activity. The ability of a valence band electron to be driven to the conduction band and produce pairs of electrons (e) and holes (h) occurs when TiO₂ NPs are exposed to UV radiation (λ 388 nm). These reactive species play a crucial role in starting a redox interaction⁷.

Titanium dioxide has been identified as a suitable photocatalytic agent in the presence of UV radiation due to its low cost, non-toxicity, chemical and physical stability, and favorable optical properties. The large band gap (3.2 eV) and the fact that it can only be stimulated by UV radiation (388 nm) to discharge electrons to the conductive band while leaving holes in the valence band are some drawbacks connected with its use. Consequently, this limits the titanium dioxide photocatalytic reaction process's ability to use sunlight or other visible light as an external excitation source. "Additionally, the high rate of hole/electron recombination in TiO₂ NPs leads to less effective photocatalysis^{8,9}".

Silver nanoparticles are one of the most promising nanomaterials for commercial uses^{10,11}. Numerous applications, such as the sterilization of medical equipment, household appliances, and the purification of water, have made use of silver nanoparticles as antimicrobial agents. "They have a wide range of applications, including electrical goods, antibacterial agents in hospitals, food storage, textile coatings, wound healing applications, and several green purposes^{12–17}". It has been examined and shown that Ag coated on titanium dioxide film using the chemical vapor deposition approach exhibits superior photocatalytic activity than other catalysts. The noble metal deposition method was widely employed to increase the photocatalytic activity of TiO₂^{18–20}. Ag cannot aggregate due to the core-shell structure. TiO₂-AgNPs showed much higher photocatalytic activity in the methylene blue degradation process when compared to pure TiO₂. According to XPS research, the TiO₂-AgNPs film has more surface hydroxyl groups than the TiO₂ film²¹. The surface OH groups were transformed into OH[•] radicals during UV irradiation, which was essential for photocatalytic activity²¹.

Core-shell composites structures, as a kind of new nanostructures, have received intense attention due to their improved physical and chemical properties over their single components, and thus many efforts have been made to synthesize such special core-shell nanostructures. The core-shell composites have many advantages as antibacterial agent, low toxicity, chemical stability. The current study aimed to synthesize and characterize silver nanoparticles and TiO₂-AgNPs core-shell and to treat the cotton fabrics with prepared nanoparticles using succinic acid as cross-linking agent in order to increase the efficiency of the textiles to UV protection and increase the self-cleaning ability to be used in producing textiles for medical uses.

Material and methods

Cotton fabrics

The unbleached long stable Egyptian cotton fabrics were obtained from Miser-El-Mehala Company for Spinning and Textile, Egypt, which were made from Giza 88 and Giza 94. The fabrics are plan weaved with a warp of 36 yarns per cm² and a weft of 30 yarns per cm². All experimental materials were under controlled atmospheric conditions of 20 ± 2 °C temperature and 65 ± 2% relative humidity.

Chemicals

Titanium (IV) isopropoxide, + 97% (C₁₂H₂₈O₄Ti) was obtained and purchased from Thermo Fisher (Kandel), Germany. Silver nitrate was purchased from Sigma Aldrich. Silver nitrate powder 99.99% was purchased from Sigma Aldrich., Soluble starch, succinic acid 99%, NaOH and H₂O₂ were purchased from PIOCHEM. Sodium hypophosphate (SHP) was obtained from Central Drug House (P) LTD New Delhi. Reactive (drimen) dye blue 2 (C₂₉H₂₀ClN₇O₁₁S₃) was purchased from ICN biomedical. INC, Germany.

Pretreatment processes

Scouring and bleaching with NaOH and H₂O₂

Non-cellulosic material on fabrics was removed by saturate fabric at 100 °C for 90 min with one liter of aqueous solution containing 40 g/L NaOH (1M) and 1% mercerol (wetting agent) with constant stirring. The liquor ratio will keep being 1:30. After scouring, the treated samples were washed under running water and dried. The scoured fabrics were bleached to remove colored materials following the recipe silicate (Na₂SiO₃·9H₂O) 3.5%, Na₂CO₃ 1% and H₂O₂ 4% for 1 h at 90 °C. All the desiring, scouring and bleaching experimental were carried out in triplicate at liquor ratio of 20:1²².

Dyeing process

The modified fabrics were dyed with 1% owf (on weight of fabric) reactive (drimen) dye with 6% (owf) at 1:50 LR (material to liquor ratio), Firstly the samples were immersed in the water and dyeing bath was warmed at 50 °C, then added salt to the dyeing bath into three times followed by adding the dye solution, then the temperature was raised to boiling through 15 min, and the dyeing was continued at this temperature for 45 min, finally the dyeing was stopped and the dyeing bath was cooled. Dyed samples were thoroughly rinsed with running water, then soaped with a solution containing 5 g/L nonionic detergent (Hostapal CV-ET) at 70 °C for 15 min, Finally, the samples were rinsed with water after washing, and left to dry in air²³.

Treatment processes

Silver nanoparticles preparation (AgNPs)

In the chemical reduction technique, alkali-dissolved starch was used as a stabilizing agent for the produced silver nanoparticles and as a reducing agent for silver ions. AgNPs were created using a high-speed homogenizer and a thermostatic water bath. Using a high-speed homogenizer, 5 g of native maize starch were completely dissolved in 80 mL of distilled water with 1.5 g of sodium hydroxide to create an alkali-dissolved starch solution. The mixture was fully dissolved before being heated to 70 °C. AgNO₃ (0.01 and 0.1 g) dissolved in 20 mL of distilled water were mixed with an aqueous solution (pH 12) of alkali-dissolved starch, drop by drop. For 60 min, the reaction mixture was continuously stirred. AgNO₃ solution was added, and shortly after, the reaction medium turned clear yellow, then brown, and finally dark brown, confirming the creation of AgNPs¹³. The colloidal solution was allowed to cool gradually to 25 °C during a 30-min period following the completion of the reaction²².

Titanium dioxide nanoparticles preparation (TiO₂NPs)

Using a magnetic stirrer, titanium tetra isopropoxide (6 mL) was combined with 1% acetic acid (2 mL). Following the addition of 56 mL of ethanol dropwise with constant stirring, the solution's pH was then corrected by adding concentrated HCl (2 mL) after 5 min. The mixture was thoroughly magnetically swirled for 45 min. after which a viscous solution was produced, indicating that TiO₂-NPs sol-gel had formed. This process was followed by 24 h of drying at 110 °C and 2 h of calcination at 450 °C in a muffle furnace²⁴.

Preparation of TiO₂-Ag core-shell nanoparticle

With a few minor modifications, the core-shell type TiO₂-Ag was made by the method of Neil et al.²⁵. In a nutshell, 30 mL of distilled water was used to sonicate 1 g of TiO₂-NPs with a 50 nm average size for 10 min. The silver nitrate solution used had the proper concentration. To create a partly stabilized dispersion, the required quantity of AgNO₃ was dissolved in deionized water (0.01–0.1 g AgNO₃ in 500 mL DW). After that, 10 g of gelatin was added to 30 mL of the TiO₂ solution and then sonicated for 10 min. The dispersions were dried at 110 °C for 24 h, and then the powder samples were subjected to a 2-h calcination process at a specified temperature of 450 °C.

Cotton fabric treatment with AgNPs and TiO₂-AgNPs

5% wt/wt succinic acid and 4% wt/wt sodium hypophosphite were mixed in the finishing bath with 100 mL volume. to crosslink Ag and TiO₂-AgNPs on cotton fabric samples. To create a dispersed solution, the prepared solution of Ag and TiO₂-AgNPs (0.01% and 0.1% OWF) was sonicated for 20 min. At room temperature, the cotton materials were submerged in the solution. The treated materials were then cured for 1.5 min. at 150 °C after being dried for 3 min at 120 °C. These remedies underwent twofold drying and curing²⁶.

Characterization of nanoparticles

UV-Vis spectroscopy

The optical properties of AgNPs and TiO₂-AgNPs were measured using a PG Instruments Ltd. T80 UV-Vis spectrophotometer in the Cotton Research Institute, Agriculture Research Centre, Egypt. At wavelengths between 300 and 700 nm, UV-Vis spectra were captured.

Transmission electron microscopy (TEM)

AgNPs and TiO₂-AgNPs were screened morphologically using transmission electron microscopy (JEM-1400, JEOL model). The imaging was captured by the electronic microscope lab at Cairo University Research Park (CURP). TiO₂-AgNPs and freshly prepared AgNPs were placed on a glow-discharged carbon grid. Then, the shape and the diameter of the nanoparticle specimens were determined by the TEM operating system.

Particle size and zeta potential

Using a Zetasizer[®] 3000 particulate size description analyzer (Malvern Instruments) in the central lab of National Institute of Standards (NIS), a complementary scientific research institute with analytical services, and by using photon interconnection spectroscopy and Laser Doppler intensity measurement, the zeta potential and particle size of the nanoparticles were ascertained, respectively. The mean hydrodynamic diameter was determined by progressive analysis after size correction was carried out three times at a 25 °C scattering angle and each correction was time-restricted for 3 min. The automated water dip cell mode was used to check the zeta potential adjustment.

Characterization of TiO₂NPs coated with cotton fabrics

Scanning electron microscopy (SEM)

The imaging of nanoparticles was captured by SEM Quanta 250 FEG (Field Emission Gun) connected to an EDX unit (energy dispersive X-ray analyses) at 30 kV accelerating voltage and 14× to 1 million magnification.

X-ray diffraction (XRD)

The nanoparticle on the textiles was examined using X-ray diffraction (XRD). CuK radiation and $\lambda = 1.5406$ Å were used to capture XRD patterns using a Bruker, D8 advance rotaflex diffraction meter. For cellulose Crystallinity, the following height ratio was used to compute the XRD crystallinity index (CIXRD), based on the peak height method for native cellulose developed by Segal et al.²⁷:

$$CI_{XRD}(\%) = \frac{I_{002} - I_{am}}{I_{002}} \times 100$$

where I_{002} was the intensity of the crystalline and I_{am} the height of the minimum.

Application of TiO₂NPs on cotton fabrics

UV protection

Using a Cary 50 solar screen transmission spectrophotometer, the transmissions of UV radiation were measured by S.A.A.S²⁸, Sun protective apparel-evaluation and classification. UPF values were determined automatically by Sharma and Singh²⁹.

The amount of UV light that passes through a substance affects its UPF. UPF measures how much longer a person can be exposed to the sun while wearing a certain garment before their skin starts to get red³⁰.

Anti-bacterial screening test

The agar plate technique³¹ was used as a qualitative test with two microorganisms, Gram-negative *Escherichia coli* (ATCC 8739) and Gram-positive *Staphylococcus aureus* (ATCC 6538), to determine if the substances had an antibacterial effect.

Agar plate method

In sterile Petri plates, the bacteriostatic activity was administered. *E. coli* and *S. aureus* 24-h broth cultures, the test organisms, were employed as inoculums. The test organisms were swabbed over the agar plates' surface using a sterile cotton swab. The core of the mat culture was gently pressed with the test textiles (fabrics coated with nanoparticles) and the control fabrics. For 18–24 h, the plates were incubated at 37 °C.

Self-cleaning property

Testing and self-cleaning finishes fabric samples that had not been treated as well as those that were loaded with Ag and TiO₂-AgNPs were stained for 15 min in a solution of basic blue dye (1% OWF), dried, and then conditioned. For 24 h, the samples were exposed to light from the sun. Fabric samples loaded with Ag and TiO₂-AgNPs as well as untreated samples had their color strength represented as a K/S value evaluated. The deterioration of the dye stains directly causes the drop in K/S values^{24,32,33}.

Strength and elongation

The force per unit linear density of the unstrained specimen is used to express the tensile stress. The National Institute for Standard (NIS-Egypt)'s Textile Metrology Department used a Shimadzu Testing Machino-Japan to test the tensile strength (Kg f) and elongation (%).

Results and discussion

Characterization of silver nanoparticles (AgNPs) and titanium oxide-silver nanoparticles (TiO₂-AgNPs)

Transmission electron microscope (TEM) of AgNPs and TiO₂-AgNPs

Figure 1a shows the TEM of the prepared AgNPs by reduction method. The size and shape of the silver nanoparticles are homogeneously monodispersed. The NPs were observed to be irregular and spherical and the size range from 10.4 to 22.2 nm. These results are in agreement with Hebeish et al.³⁴, who observed that the TEM of AgNPs has a spherical morphology and the size of AgNPs lies between 7.53 and 21.060 nm.

Figure 1b shows the TEM of the TiO₂-Ag core-shell. It is evident that the TiO₂ serves as the shell and the silver nanoparticles serve as the core; both have uniform hexagonal shapes with size range from 39.7 to 74.6 nm. The average core size is 11.54 nm, and the average shell thickness is 94.5 nm. These findings concur with those of

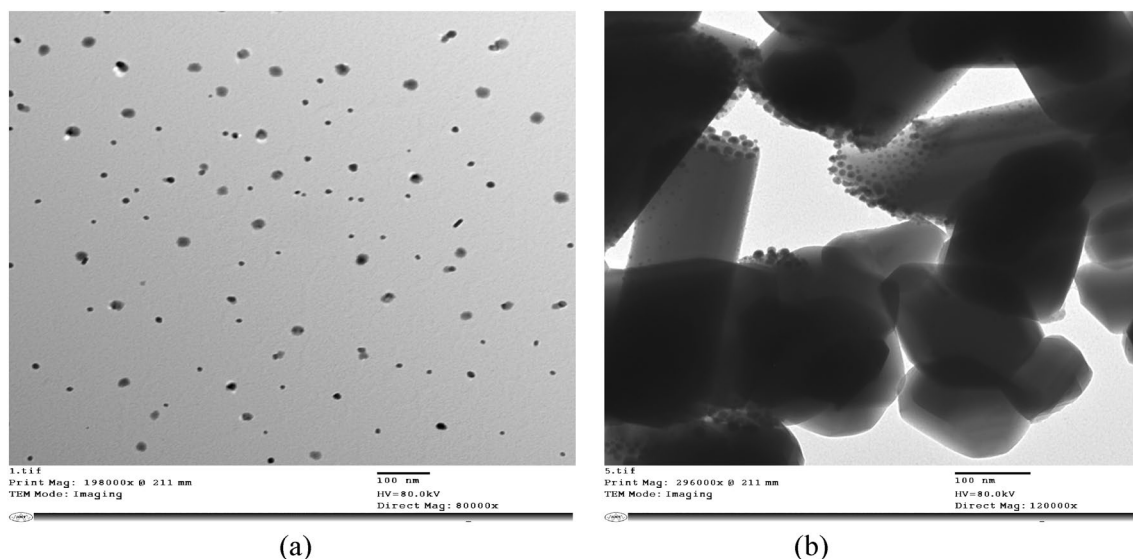


Figure 1. Transmission electron microscope micrograph of (a) AgNPs and (b) TiO₂-AgNPs.

Yang et al.³⁵ and Min et al.³⁶, they obtained that TEM images of Ag-TiO₂ core-shell nanoparticles have Ag cores with diameters of 50–100 nm generated by a polyol-thermal approach.

UV-Vis spectrum of AgNPs and TiO₂-AgNPs

The optical characteristics of nanoparticles were evaluated using a UV-Vis spectrometer. The UV-Vis spectra for the core-shell architectures of AgNPs and TiO₂-AgNPs are shown in Fig. 2. When coated with TiO₂ nanoparticles, the wavelength absorbance peak of the Ag nanoparticles, which is centered at 440 nm (Fig. 2a), is attenuated. It also moved in the absorption wavelength area (316 nm) in Fig. 2b, which is comparable to that of Ag-TiO₂NPs. These results agree with Yang et al.³⁵ and Min et al.³⁶ which found that the wavelength peak of TiO₂-AgNPs at 320 nm.

Energy dispersive X-ray spectra (EDX) of AgNPs and TiO₂-AgNPs

The composition of the Ag and TiO₂-Ag nanoparticles was determined by energy dispersive X-ray (EDX). The produced AgNPs were subjected to chemical analysis using EDX, which verified the presence of both Ag and the alkali-dissolved starch coating the AgNPs. Metallic silver nano-crystals typically exhibit an optical observation peak at about 2.984 keV because of surface plasmon resonance.

The Ag nanoparticles are also demonstrated by the EDX spectra to be in the metallic state, devoid of Ag₂O production and other contaminants. Figure 3a provided evidence of the high concentration of powdered AgNPs. AgNPs have a molecular ratio of 100%. These findings concur with those of Hebeish et al.³⁴, who found that surface plasmon resonance causes metallic silver nanocrystals to typically exhibit an optical observation peak at 3 keV. The spectrum of TiO₂-AgNPs, as depicted in (Fig. 3b), clearly shows prominent peaks of the components Ag, Ti, and O, demonstrating that the TiO₂ layer successfully coated the Ag nanoparticles. Ag, Ti, and O have molecular ratios of 0.95%, 67.01%, and 32.04%, respectively according to Min et al.³⁶, which found that the Ag, Ti, and O all exhibit prominent peaks in the spectrum, indicating that the TiO₂ layer coating of the Ag nanoparticles was effective.

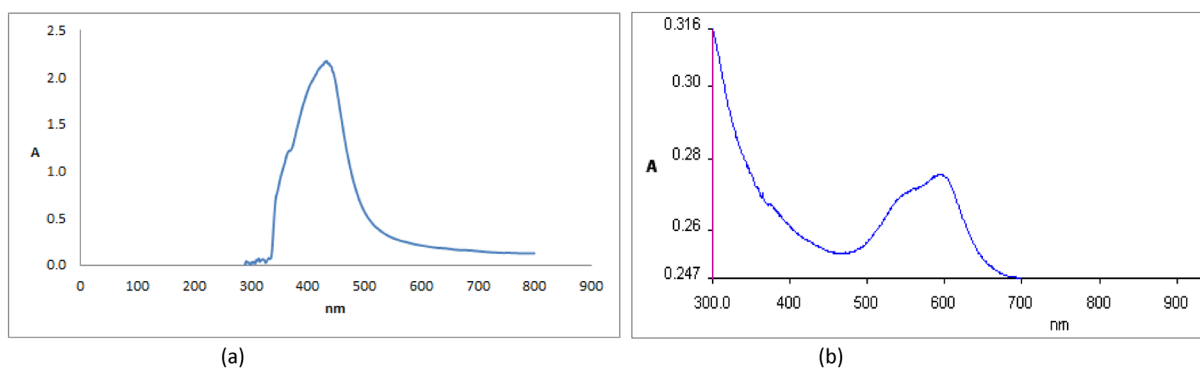
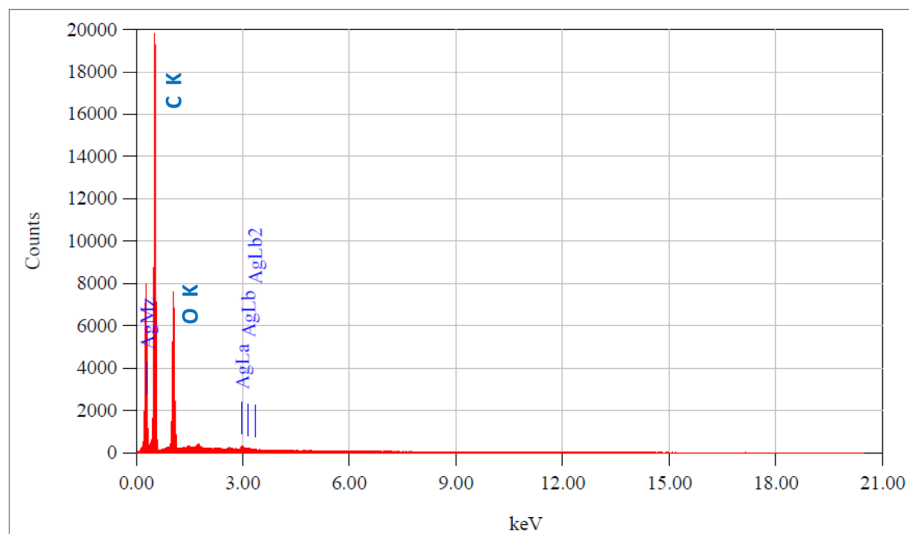
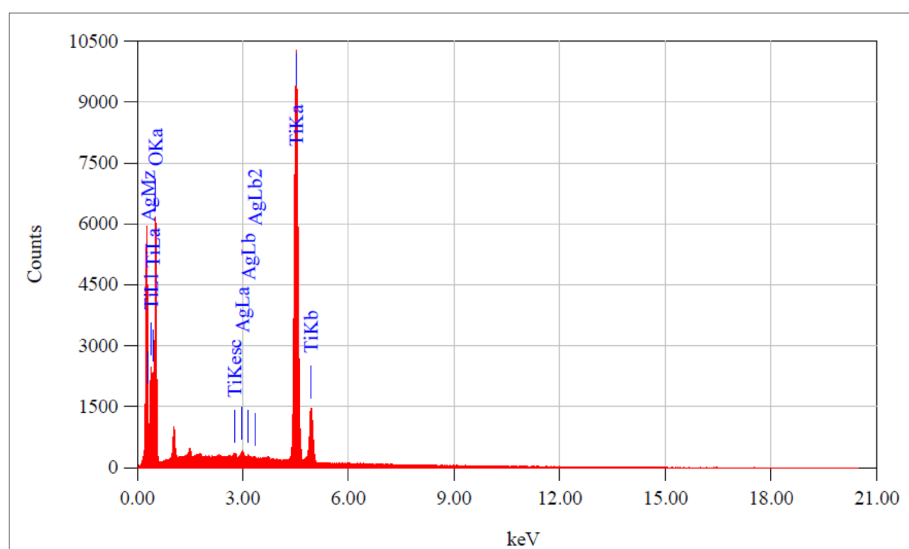


Figure 2. UV-Vis absorption spectra of (a) AgNPs and (b) TiO₂-Ag core-shell nanoparticle absorbance.



(a)



(b)

Figure 3. EDX spectra of (a) AgNPs and (b) TiO₂-Ag core-shell nanoparticle.

Particle size (PS) and zeta potential (ZP)

The size and charge of nanomaterials can be determined by zetasizer. Figures 4 and 5 show the particle size distribution and zeta potential of AgNPs and TiO₂-AgNPs core-shell. It's clear in Fig. 4a,b the size distribution of the colloidal AgNPs with a concentration of 0.01% was found at 120 nm, and the ZP value was determined to be -20.8 mV. The presence of hydroxyl groups from starch molecules structure cap the produced AgNPs, which results in their negative ZP according to Hebeish et al.³⁴. The average size and zeta potential of core-shell nanoparticle TiO₂-AgNPs are presented in Fig. 5a,b which show The size of the colloidal TiO₂-AgNPs is 140.2 nm and the ZP of these colloidal is -30.7 mV). These results are in agreement with Cosgrove³⁷, which found that the solutions with zeta potential above $+20$ mV or below -20 mV are stable.

Cotton fabrics characterization

The main aim of this work is to apply AgNPs and TiO₂-AgNPs to cotton fabric (G88 and G94) as an antibacterial finishing agent, UV protection, and self-cleaning agent. The treated cotton fabric was then assessed.

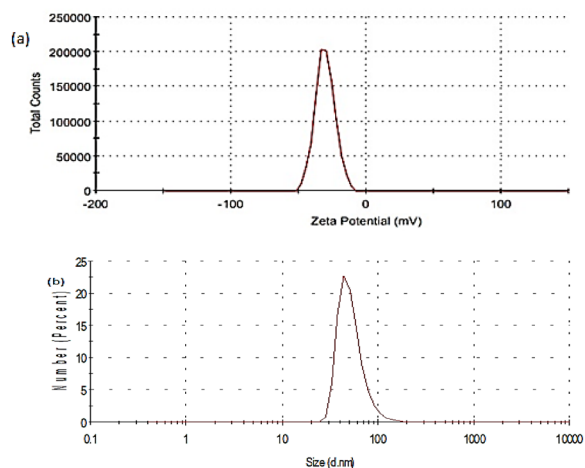


Figure 4. (a) Zeta potential and (b) size distribution by number of AgNPs.

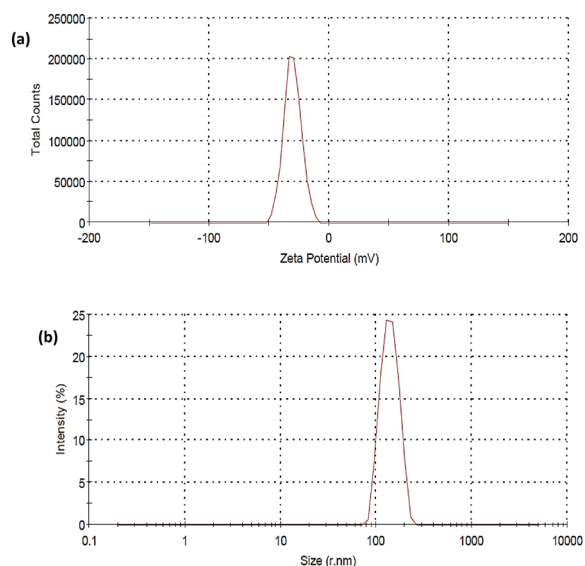


Figure 5. (a) Zeta potential and (b) size distribution by number of TiO₂-AgNPs core-shell.

Scanning electron microscope (SEM)

Investigations were conducted into the morphological structure of cotton textiles treated with AgNPs and TiO₂-AgNPs, respectively, and compared to untreated cotton fabric. Figure 6 depicts the surface structure of cotton fabric both before and after treatment. Figure 6a shows that the cotton fabric is untreated and has smooth sheaths around the tangled textiles with no discernible particles accumulated on the surface. As a result of the textiles being treated with prepared nanomaterials (AgNPs and TiO₂-AgNPs), (Fig. 6b,c) exhibits a rough surface. To better understand the situation, a high-magnification SEM image of the treated textiles is obtained to show the morphology of the deposited particles from the two distinct materials (Fig. 6b,c). The particles that developed on the surface of textiles seem to be spherical at this high SEM magnification, and the nanoparticles are evenly spread over the fiber surface. these results in agreement with Yang et al.³⁸ and El-Naggar et al.³⁹, they found that the morphological structure analyses confirm that the cotton fabric's inherent properties allow nanoparticles to be spontaneously captured and settled onto the fabric.

X-ray diffraction studies

The crystalline structure of the cotton coated by AgNPs and TiO₂-AgNPs was examined using the XRD pattern. Figures 7a-c and 8a-c show the XRD of cotton fabric G88 and G94, respectively. All samples' XRD spectra show two distinct peaks at 2 angles of 16.450 and 22.640 that originate from cotton as the primary substrate (control sample in Figs. 7a, 8a). The presence of AgNPs on the treated textiles (Figs. 7b, 8b) can be confirmed by characterization peaks at 2θ angles 34.21°, 42.580°, and 73.69°. Characterization peaks at 2θ angles in the spectra of the cotton samples treated with TiO₂-Ag nanocomposites (Figs. 7c, 8c) provide evidence for their existence,

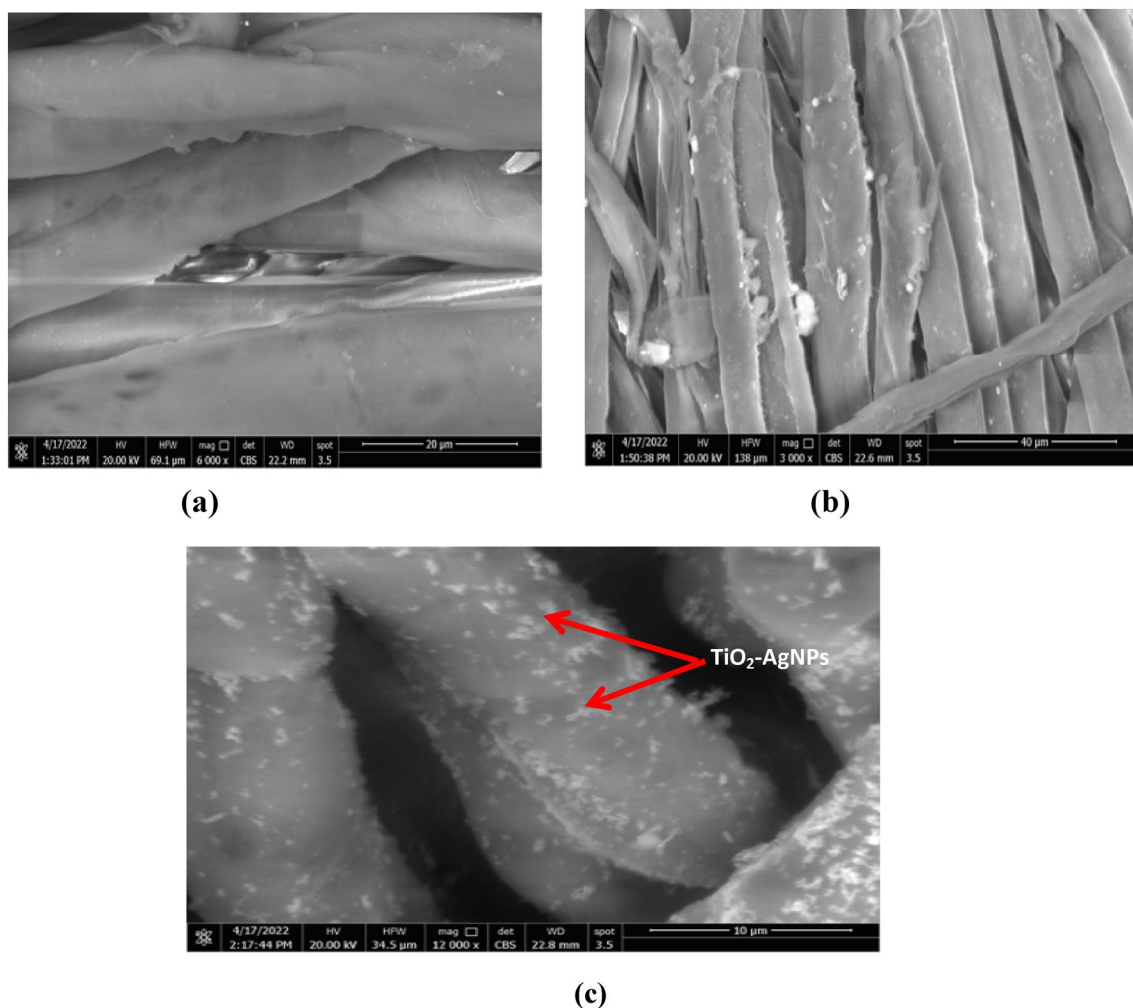


Figure 6. SEM of cotton fabric samples coated with TiO_2 -Ag core-shell (a) untreated cotton (b) treated with AgNPs (c) treated with TiO_2 -AgNPs core-shell.

25.25°, 25.98°, 27.40°, 34.51°, 35.89°, 54.25° and 68.84° and in agreement with Yang et al.³⁶, who found that the XRD pattern of Ag/ TiO_2 and exhibits characteristic peaks at 2θ 25.37°, 48.12°, 53.97° and 55.10°, corresponding to (101), (200), and (105) planes, respectively, which belong to typical anatase- TiO_2 materials. The crystallinity index of the fabrics treated with AgNPs was increased from 76.40 to 92.33%. On the other hand, the treated fabrics with core-shell Ag- TiO_2 was 81.35% in the case of G88, and the crystallinity index of G94 was increased from 75.42% to 77.33 in concentration of 0.1% AgNPs but decreased in the case of core-shell TiO_2 -Ag to 71.93%.

UV protection property

It is generally known that prolonged exposure to UV radiation may cause serious damage to human skin. These UV rays have been connected to skin cancer development. The UV-Visible spectrophotometer was used to measure the treated cotton fabric's capacity to block UV radiations or UPF.

The results in Table 1 and Fig. 9 show the application of AgNPs and TiO_2 -AgNPs core-shell nanoparticles with succinic acid / SHP cross linking agents in different concentrations (0.01% and 0.1% OWF). Table 2 displays the UVA rays transmitted for cotton fabrics in the UVA (320–400 nm) and UVB (280–320 nm) regions (abbreviated as TUVB and TUVB). UV transmission on treated cellulose fabrics (G88 and G94) was significantly lower than on untreated cellulose fabrics, which led to an increase in the UPF (Ultraviolet Protection Factor) value that was automatically calculated, this number indicates how long a person can stay in the sun while wearing protective clothes before their skin starts to get red. The results show that G88 indicates a higher UPF value followed by G94 and core-shell nanoparticles give high results compared with silver only owing to the dual effect of AgNPs and TiO_2 -Ag nanoparticles. TiO_2 -Ag nanoparticles, which have a high photocatalytic activity, a low density, and an excellent resistance to UV radiation, can be used as an example of this phenomenon. All treated cotton fabrics give excellent UV protection. These results in agreement with Ali et al.⁴⁰ and Jafari-Kiyani et al.⁴¹ they found that after functional finishing of cotton by titanium dioxide nanoparticles, the transmittance values of the sample decreased significantly because of the UV absorption ability of TiO_2 -NPs. Moreover, the UV-blocking activity of the nanocomposites-treated fabrics was improved by the presence of silver nanoparticles on the surface of cotton fabrics. Due to the UV reflection ability of the AgNPs, coating cotton fabric with TiO_2 -Ag nanocomposites

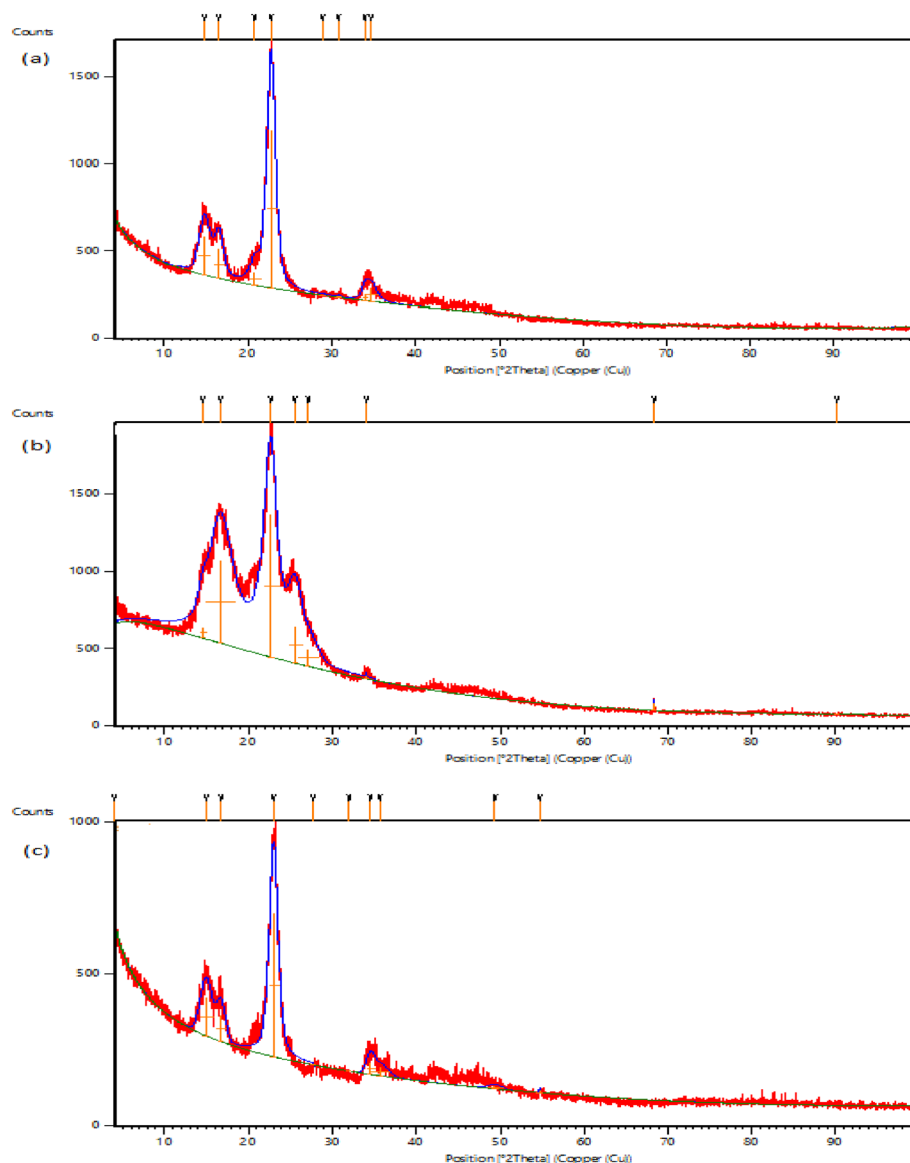


Figure 7. XRD studies of cotton fabric samples G88 (a) untreated cotton (b) treated with AgNPs (c) treated with Ag-TiO₂NPs.

led to a more significant decrease in UV transmittance values⁴⁰. The UPF value of the blank cotton sample was 11.12. An UPF value of 15 indicated no protection against transmittance of UV radiation through fabric onto skin. The UPF values of the treated cotton samples were measured to be 244.11, 263.23, 265.18 and 267.01 for TiO₂ nanoparticles, yellow-nanocomposite, blue-nanocomposite, and brown-nanocomposite, respectively. Therefore, results confirmed the excellent UV-blocking activity⁴¹.

Transmitted UVA (320–400 nm) and UVB (280–320 nm) regions which were expressed as TUV_A and TUV_B. UPF: UV protection factor TUV Transmitted UV radiation %. Transmitted UVA (320–400 nm) and UVB (280–320 nm) regions which were expressed as TUV_A and TUV_B. UPF: UV protection factor TUV transmitted UV radiation %.

Self-cleaning of fabrics

The data indicates that cotton fabrics degraded 99% of methylene blue in 24 h by photocatalysis under UV and solar irradiation, conforming to self-cleaning properties. Figure 10 shows the self-cleaning and degradation of the dye on the blank and treated cotton fabric (G88 and G94) with different concentrations of AgNPs and TiO₂-AgNPs core-shell with different concentrations (0.01% and 0.1% OWF). A concentration of 0.01% nanoparticles resulted in the degradation of 99.9% of methylene blue. Titanium dioxide nanoparticles were used to initiate the photocatalytic breakdown of dye stains using the energy of UV radiation. By exposing the stained samples to standard laboratory settings, titanium dioxide's photocatalytic abilities changed the stains' molecular structure, making them colorless. The elimination of MB dye stains from all treated samples was found to be highly effective. The characteristics of the finished fabrics were not considerably decreased even after 50 washing

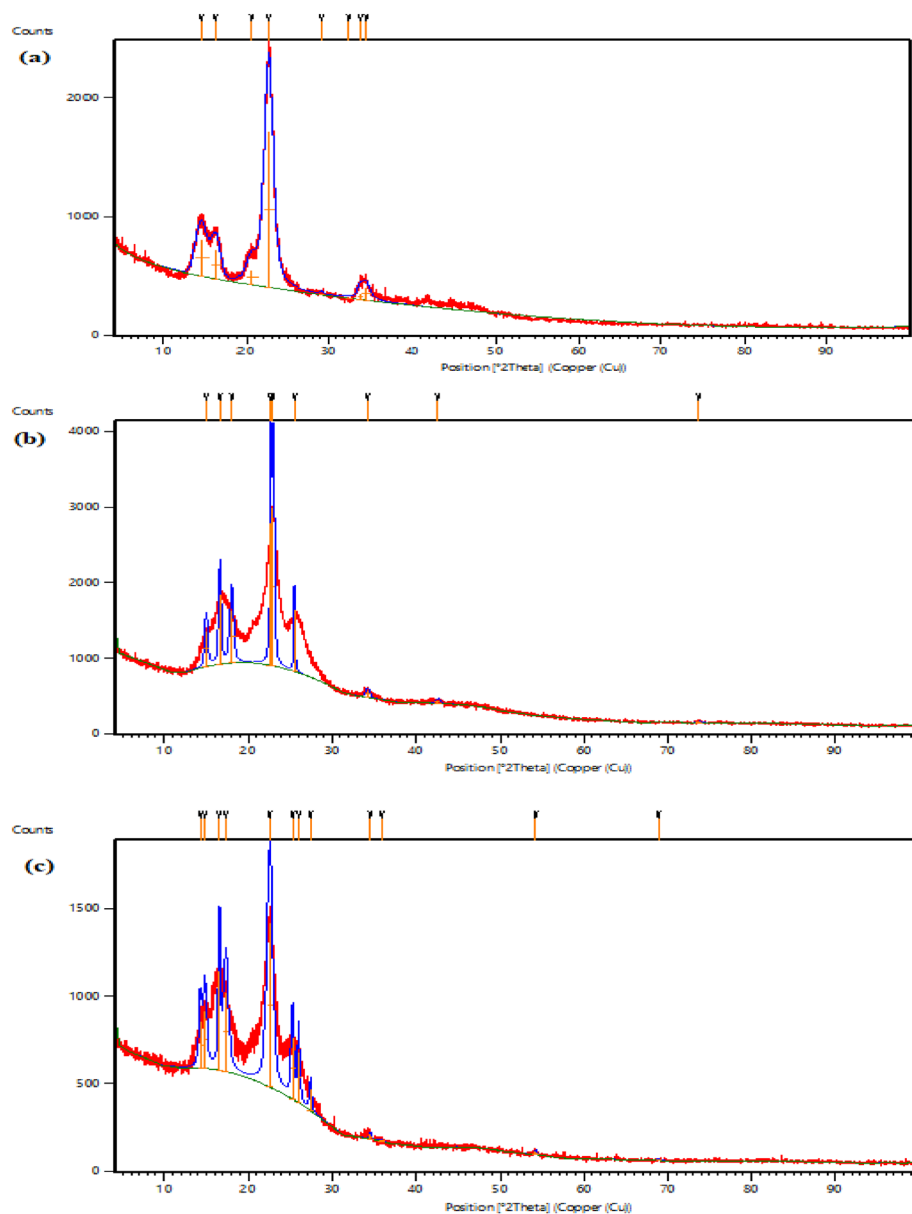


Figure 8. XRD studies of cotton fabric samples G94 (a) untreated cotton (b) treated with AgNPs (c) treated with Ag-TiO₂NPs.

Varieties	Giza 94			Giza 88		
	UPF value	TUVA	TUVB	UPF value	TUVA	TUVB
Control	33.33 ± 0.88	7.29	3.03	35.86 ± 2.20	5.6	3.15
AgNPs 0.01%	48.25 ± 1.18	2.98	2.09	50.04 ± 1.16	1.65	2.06
AgNPs 0.1%	62.30 ± 1.17	2.59	1.8	63.44 ± 1.16	3.05	2.75
TiO ₂ -AgNPs 0.01%	79.00 ± 1.16	2.56	0.4	86.06 ± 1.16	3.09	0.99
TiO ₂ -AgNPs 0.1%	117.30 ± 1.20	0.92	0.51	129.23 ± 1.18	2.74	0.58

Table 1. Effect of AgNPs and TiO₂-AgNPs core-shell with succinic acid on UV protection of cotton fabrics. Transmitted UVA (320–400 nm) and UVB (280–320 nm) regions which were expressed as TUVA and TUVB. UPF UV protection factor TUV transmitted UV radiation %. Transmitted UVA (320–400 nm) and UVB (280–320 nm) regions which were expressed as TUVA and TUVB. UPF UV protection factor TUV transmitted UV radiation %

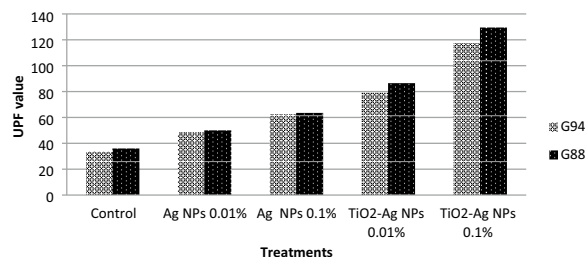


Figure 9. Effect of AgNPs and TiO₂-AgNPs core-shell with succinic acid on UV protection of cotton fabrics.

UV protection	UPF classification	transmitted UV radiation (%)
Excellent	40, 45, 50, 50+	≤2.5
Very good	25, 30, 35	4.1–2.6
Good	15, 20	6.7–4.2
Non-ratable	0, 5, 10	>6.7

Table 2. UV protection and classification according to²⁸.

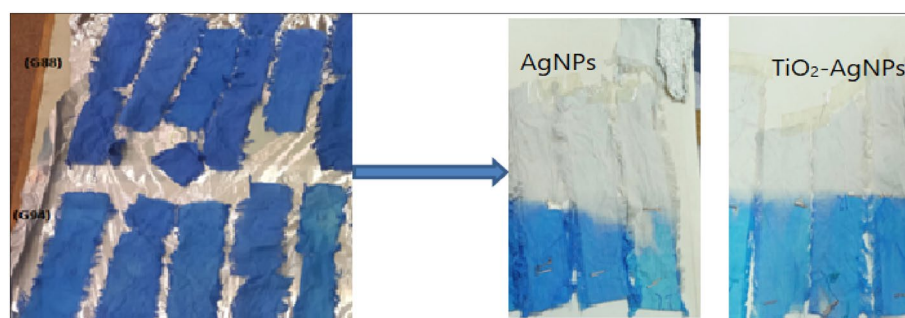


Figure 10. Images of degradation of methylene blue under UV radiation at 24 h by AgNPs and TiO₂-AgNPs core-shell on cotton fabrics.

cycles⁴². These findings support those of Norouzi and Maleknia⁴³, Sami and Barakat⁴⁴ and Abou-Okeil et al.⁴⁵ who found that 2% of TiO₂ nanoparticles are almost sufficient to give enough self-cleaning. Alvarez-Ampanán et al.⁴⁶ found that the TiO₂-NPs functionalized cotton fabrics degraded 99% of methylene blue in 60 min by photo catalysis under UV and solar irradiation conforming self-cleaning properties.

Anti-bacterial properties

Tables 3 and 4 show the antibacterial properties of treated and untreated textiles with AgNPs and TiO₂-Ag core-shell nanoparticles against common harmful bacteria like *E. coli* and *S. aureus*. It has been demonstrated that the development of germs is unaffected by untreated cotton cloth. The development of the investigated microorganisms is significantly inhibited in the meanwhile by the AgNPs-treated cotton samples. Contrarily, the antimicrobial effects of textiles treated with TiO₂-AgNPs had a greater impact against pathogenic bacteria,

Varieties	G88	G94
Zone inhibition (mm)		
Control	0 ± 0.00	0 ± 0.00
AgNPs 0.01%	8 ± 1.53	7 ± 1.53
AgNPs 0.1%	12 ± 2.08	10 ± 1.53
TiO ₂ -AgNPs 0.01%	14 ± 1.53	11 ± 1.73
TiO ₂ -AgNPs 0.1%	17 ± 1.53	13 ± 1.53

Table 3. Effect of AgNPs and TiO₂-AgNPs core-shell with different concentration on zone inhibition of *E. coli*.

Varieties	G88	G94
Zone inhibition (mm)		
Control	0 ± 0.00	0 ± .00
AgNPs 0.01%	11 ± 1.53	10 ± 1.53
AgNPs 0.1%	15 ± 2.73	12 ± 2.52
TiO ₂ -AgNPs 0.01%	16 ± 4.16	13 ± 1.16
TiO ₂ -AgNPs 0.1%	20 ± 2.52	15 ± 3.61

Table 4. Effect of AgNPs and TiO₂-AgNPs core-shell with different concentrations on zone inhibition of *Staphylococcus aureus*.

supporting the significance of TiO₂NPs when bound to AgNPs. *S. aureus* has a larger inhibition zone than *E. coli*, which is lower.

It observed from the results that the response of G88 which recorded higher results against the pathogenic bacteria due to the genetic properties of the varieties. TiO₂NPs may increase AgNPs' beneficial ability to enter the bacterial cell wall and connect to DNA and peptide groups, which in turn damages the cell wall, obstructs bacterial reproduction, and ultimately kills microorganisms^{39,47,48}. Silver nanoparticles can stop infections by gathering in cell wall pores and causing cell membrane hydrolysis. These findings support those of Li et al.⁴⁹ and El-Naggar et al.³⁹, they discovered that using of TiO₂-AgNPs at a high concentration (0.6 g) is more advantageous for producing better antibacterial cotton.

Cotton fabric's mechanical properties

Tensile elongation and strength

The Tensile elongation and strength data of the samples were collected in Table 5. Silver nanoparticles treatment with two different concentrations (0.01% and 0.1%) and succinic acid caused a change in fabric strength accompanied by a decrease in the concentration of Giza 88 which was recorded by 420.00 in the control sample decreased to 350.66 under concentration 0.01% then followed slightly increased by concentration 0.1% recorded of 360.00. In The case of Giza 94 also with decreasing in the concentration was recorded from 365.46 in the control sample to 291.06 in concentration of 0.01% followed by an increase under the concentration of 0.1% to 342.00, on the other hand, the case of core-shell TiO₂-Ag in all varieties of the strength of the fabrics decrease again in the case of TiO₂-Ag with concentration 0.01%. This results from succinic acid's acidity and the influence of TiO₂, which reduced the tensile strength because TiO₂ nanoparticles have greater oxidation and photocatalysis, and macromolecule linkages partially disintegrate under UV radiation. Through the development of a terminal group of fibrous formless molecular chains and the degradation of fibrous super-molecular structure, this ultimately reduced the fibrous macroscopic mechanical characteristics and caused damage to the fiber. According to Wang, et al.⁵⁰, this increased in the case of 0.1 TiO₂-Ag in all varieties as a result of the fabric's inter-yarn voids being filled, which caused friction between the yarns and made them resistant to stretching. However, with every increase in strength, fabric elongation decreases in the length of the specimen.

AgNPs and their core-shell nanoparticles treated with two different concentrations and succinic acid 5 g/L led to a decrease in the tensile strength which caused an increase in fabric elongation % in variety G94 which was increased by increasing the concentration relative to control that recorded 19.40, and increase in concentration (0.01% and 0.1% to 27.29 and 26.24) respectively, while the core-shell of nanoparticle (TiO₂-Ag) with concentration (0.01% and 0.1%) the fabric elongation was decreased gradually recorded (22.32 and 24.11). The fabric elongation of G88 was increased in concentration (0.01% and 0.1%) and then decreased in the TiO₂-Ag decreased the elongation of fabric owing to succinic acid's acidity and TiO₂ which have photocatalytic properties. These results in agreement with Akhavan et al.⁵¹ who found that the loss on tensile strength fabric could be related to the ultrasonic irradiation and/or cleavage of the cellululosic chains by acid hydrolysis.

TiO₂ is one of the most effective photocatalytic materials, nano TiO₂, is highly active, and has strong oxidizing strength and long-term stability. Electrons in nano TiO₂ are excited from the valence band to the conduction

Treatment	T.S		Elongation	
	G94	G88	G94	G88
Control	365.46 ± 0.87	420.00 ± 1.16	19.40 ± 1.33	18.13 ± 3.06
AgNPs 0.01%	291.06 ± 1.16	350.66 ± 1.16	27.29 ± 1.19	25.11 ± 1.16
AgNPs 0.1%	342.00 ± 1.16	360.00 ± 1.16	26.24 ± 1.18	23.07 ± 1.16
Ag-TiO ₂ NPs 0.01%	330.26 ± 1.19	341.20 ± 1.17	22.32 ± 1.20	21.16 ± 1.17
Ag-TiO ₂ NPs 0.1%	386.26 ± 1.19	473.00 ± 1.16	24.11 ± 1.16	22.02 ± 1.16

Table 5. Tensile strength and elongation of cotton fabrics G88 and G94. (T.S) Tensile strength as (N/f) elongation as % relative to control.

band when exposed to ultraviolet light with wavelengths less than 385 nm. Hydroxyl radicals are formed when the positive hole in the valence band reacts with water or hydroxide ions adsorbed on the surface, Superoxide ions are formed when an electron in the conduction band reduces O_2 . These two highly reactive species can decompose a wide range of organic materials, including bacteria. With the aid of a binder, the TiO_2 nanoparticles were effectively incorporated into cotton and maintained their antimicrobial activity for up to 10 washes^{52–54}. TiO_2 nanoparticles is the strong oxidizability of the photocatalyst, the fiber macromolecules can be easily broken so that the end group number of molecular chain of amorphous part of fiber increases and the super molecular structure of the fiber weakens. This finally results in a decrease in macro-mechanical property of the fibers. Thus, making the nanometer particle evenly disperse onto textile and tightly combining it with nanometer material and fiber shall be crucial during development and application for nanometer composite multifunctional textile^{55,56}.

Heterogeneous photocatalysis is predicated on the idea that when a semiconductor, usually TiO_2 , is absorbed, photon energy either equals or surpasses its band gap ($h\nu \geq E_g$). Highly reactive oxygen species (ROS) are produced when the electron-hole pairs that are created participate in a sequence of oxidation-reduction events with species adsorbed on the TiO_2 surface, as seen in Fig. 11. to produce oxygen species that are very reactive (ROS). These organisms interact with the microbes or adsorbed organic compounds on the TiO_2 surface, causing them to break down into dangerous substances like CO_2 and H_2O . Nonetheless, electrons and holes have shorter half-lives, which frequently limits their availability for involvement in redox processes. Furthermore, energy released in the form of waste heat or light and a drop in process efficiency are signs of the recombination event. How can the lifespan of electrons and holes in TiO_2 photocatalyst be extended before recombination occurs? is the challenge^{57–62}.

One of the effective methods for delaying the recombination of electron-hole pairs and shifting the light absorption range of TiO_2 photocatalyst toward visible light is doping the material with silver nanoparticles^{63,64}. Silver nanoparticles have two unique effects that increase TiO_2 photocatalytic activity:

1. Serving as an electron trap to collect electrons moved from the TiO_2 semiconductor's conduction band and move them to oxygen, whereupon they transform into superoxide radicals. Hydroxyl radicals are formed when water molecules combine with photogenerated holes in the valence band that is still present on TiO_2 . These free radicals are useful for inhibiting microorganisms and photocatalytically oxidizing contaminants (Fig. 12)⁶⁵.
2. Producing the surface plasmon resonance (SPR) phenomenon, which simultaneously increases TiO_2 photocatalytic effectiveness and expands light absorption into the visible light area^{66,67}.

Conclusions

In the current study, it was intended to synthesize functionalized AgNPs, and TiO_2 -AgNPs in straightforward, cost-effective, and reliable ways. AgNPs, and TiO_2 -AgNPs were prepared to be used in the treatment of cotton fabrics to improve their UV protection properties, self-cleaning, elongation and strength, as well as the

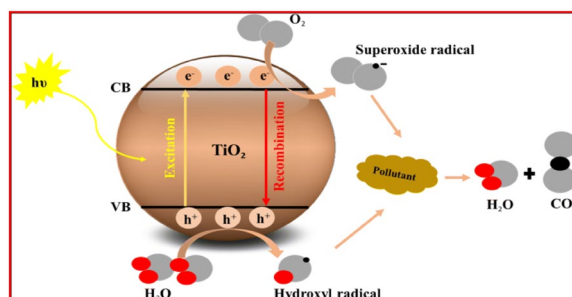


Figure 11. TiO_2 semiconductor photocatalysis principle⁶³.

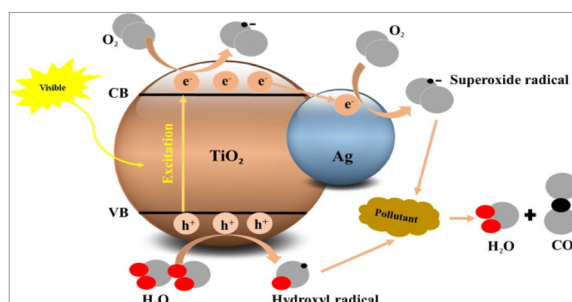


Figure 12. Photocatalytic activity of Ag/ TiO_2 photocatalyst⁶³.

antimicrobial activities to use the produced textiles for medical and laboratory uses and to increase protection for medical workers. The nanoparticles that had been created were confirmed to have a small size and good distributions. Additionally, SEM, zetasizer, and XRD analyses were used to study the chemical reactions between AgNPs and TiO₂-AgNPs and the cotton fabric's succinate and cellulose chains. In comparison to the untreated cotton fabrics, treated cotton textiles showed improvements in surface roughness, elongation (%), and tensile strength. Functionalizing the fabric with TiO₂-AgNPs led to an exceptional enhancement of treated cotton textiles. Additionally, cotton fabrics treated with TiO₂-AgNPs have higher UPF ratings than fabrics treated with AgNPs and untreated cotton fabrics. Superior inhibitory activity was achieved by the antimicrobial cotton fabrics functionalized with TiO₂-AgNPs against pathogenic bacteria including *S. aureus* and *E. coli*. The acquired results demonstrated that the AgNPs and TiO₂-AgNPs covering offered UV protection and antibacterial action. This may be due to the nanoparticles' small size, which allows them to permeate materials with ease, as well as the beneficial effects of the crosslinking agent. As a result, cotton fabric treated with TiO₂-AgNPs can be thought of as a versatile finishing agent effective for textiles used in sports and medicine.

Data availability

All data generated or analysed during this study are included in this published article.

Received: 5 November 2023; Accepted: 8 March 2024

Published online: 05 April 2024

References

1. Yasin, S. & Sun, D. Propelling textile waste to ascend the ladder of sustainability: EOL study on probing environmental parity in technical textiles. *J. Clean. Prod.* **233**, 1451–1464. <https://doi.org/10.1016/j.jclepro.2019.06.009> (2019).
2. Danihelová, A. *et al.* Usage of recycled technical textiles as thermal insulation and an acoustic absorber. *Sustainability* **11**(10), 2968. <https://doi.org/10.3390/su11102968> (2019).
3. Riaz, S., Ashraf, M., Hussain, T., Hussain, M. T. & Younus, A. Fabrication of robust multifaceted textiles by application of functionalized TiO₂ nanoparticles. *Colloids Surf. A Physicochem. Eng. Aspects* **581**, 123799. <https://doi.org/10.1016/j.colsurfa.2019.123799> (2019).
4. Syafiuddin, A. Toward a comprehensive understanding of textiles functionalized with silver nanoparticles. *J. Chin. Chem. Soc.* **66**(8), 793–814. <https://doi.org/10.1002/jccs.201800474> (2019).
5. Butola, B. S. & Verma, D. Facile synthesis of chitosan-silver nanoparticles onto linen for antibacterial activity and free-radical scavenging textiles. *Int. J. Biol. Macromol.* **133**, 1134–1141. <https://doi.org/10.1016/j.ijbiomac.2019.04.186> (2019).
6. Tudu, B. K., Sinhamahapatra, A. & Kumar, A. Surface modification of cotton fabric using TiO₂ nanoparticles for self-cleaning, oil–water separation, antistain, anti-water absorption, and antibacterial properties. *ACS Omega* **5**(14), 7850–7860. <https://doi.org/10.1021/acsomega.9b04067> (2020).
7. Farner Budarz, J. *et al.* Influence of aqueous inorganic anions on the reactivity of nanoparticles in TiO₂ photocatalysis. *Langmuir* **33**(11), 2770–2779. <https://doi.org/10.1021/acs.langmuir.6b04116> (2017).
8. Mishra, A., Mehta, A. & Basu, S. Clay supported TiO₂ nanoparticles for photocatalytic degradation of environmental pollutants: A review. *J. Environ. Chem. Eng.* **6**(5), 6088–6107. <https://doi.org/10.1016/j.jece.2018.09.029> (2018).
9. Deshmukh, S. P., Patil, S. M., Mullani, S. B. & Delekar, S. D. Silver nanoparticles as an effective disinfectant: A review. *Mater. Sci. Eng. C* **97**, 954–965. <https://doi.org/10.1016/j.msec.2018.12.102> (2019).
10. Fadlilah, D. R. *et al.* Enhancement of antibacterial properties of various polymers functionalized with silver nanoparticles. *Biointerface Res. Appl. Chem.* **10**(3), 5592–5598. <https://doi.org/10.33263/BRIAC0103.592598> (2020).
11. Ratnasari, A., Endarko, E. & Syafiuddin, A. A green method for the enhancement of antifungal properties of various textiles functionalized with silver nanoparticles. *Biointerface Res. Appl. Chem.* **10**, 7284–7294. <https://doi.org/10.33263/BRIAC106.72847294> (2020).
12. Abdallatif, A. M., Hmam, I. & Ali, M. A. Impact of silver nanoparticles mixture with NAA and IBA on rooting potential of *Psidium guajava* L. stem cuttings. *Egypt. J. Chem.* **65**(132), 1119–1128. <https://doi.org/10.21608/ejchem.2022.155986.6751> (2022).
13. Abo-El-Yazid, Z. H., Ahmed, O. K., El-Tholoth, M. & Ali, M. A. S. Green synthesized silver nanoparticles using *Cyperus rotundus* L. extract as a potential antiviral agent against infectious laryngotracheitis and infectious bronchitis viruses in chickens. *Chem. Biol. Technol. Agric.* **9**(1), 1–11. <https://doi.org/10.1186/s40538-022-00325-z> (2022).
14. Ahmed, M. *et al.* Proximate analysis of *Moringa oleifera* leaves and the antimicrobial activities of successive leaf ethanolic and aqueous extracts compared with green chemically synthesized Ag-NPs and crude aqueous extract against some pathogens. *Int. J. Mol. Sci.* **24**(4), 3529. <https://doi.org/10.3390/ijms24043529> (2023).
15. Ahmed, M. *et al.* Studying the antioxidant and the antimicrobial activities of leaf successive extracts compared to the green-chemically synthesized silver nanoparticles and the crude aqueous extract from *Azadirachta indica*. *Processes* **6**, 1644. <https://doi.org/10.3390/pr11061644> (2023).
16. El-Baz, Y. G. *et al.* An analysis of the toxicity, antioxidant, and anti-cancer activity of cinnamon silver nanoparticles in comparison with extracts and fractions of *Cinnamomum cassia* at normal and cancer cell levels. *Nanomaterials* **13**(5), 945. <https://doi.org/10.3390/nano13050945> (2023).
17. Su, T. L., Chen, T. P. & Liang, J. Green in-situ synthesis of silver coated textiles for wide hygiene and healthcare applications. *Colloids Surf. A Physicochem. Eng. Aspects* **657**, 130506. <https://doi.org/10.1016/j.colsurfa.2022.130506> (2023).
18. Balek, V. *et al.* Characterization of nitrogen and fluorine co-doped titania photocatalyst: Effect of temperature on microstructure and surface activity properties. *J. Phys. Chem. Solids* **68**(5–6), 770–774. <https://doi.org/10.1016/j.jpcs.2007.01.028> (2007).
19. Li, J., Xu, J., Dai, W. L., Li, H. & Fan, K. Direct hydro-alcohol thermal synthesis of special core-shell structured Fe-doped titania microspheres with extended visible light response and enhanced photoactivity. *Appl. Catal. B Environ.* **85**(3–4), 162–170. <https://doi.org/10.1016/j.apcatb.2008.07.008> (2009).
20. Hirakawa, T. & Kamat, P. V. Charge separation and catalytic activity of Ag-TiO₂ core-shell composite clusters under UV-irradiation. *J. Am. Chem. Soc.* **127**(11), 3928–3934. <https://doi.org/10.1021/ja042925a> (2005).
21. Sfamini, S. *et al.* Inorganic finishing for textile fabrics: Recent advances in wear-resistant, UV protection and antimicrobial treatments. *Inorganics* **11**(1), 19. <https://doi.org/10.3390/inorganics11010019> (2023).
22. Hebeish, A. R. & Mashoor, K. M. Effect of pretreatments on some physical and chemical properties of cotton cellulose before and after dyeing during irradiation part I: Effect of pretreatment on the photo degradation of cotton. *Am. Dyestuff Rep.* **60**, 39–42 (1970).
23. Wang, J., Freeman, H. S. & Claxton, L. D. Synthesis and mutagenic properties of 4, 4'-diamino-p-terphenyl and 4, 4'-diamino-p-quaterphenyl. *Color. Technol.* **123**(1), 34–38. <https://doi.org/10.1111/j.1478-4408.2006.00058.x> (2007).

24. Abou-Okeil, A., Eid, R. A. A. & Amr, A. Multi-functional cotton fabrics using nano-technology and environmentally friendly finishing agents. *Egypt. J. Chem.* **60**, 161–169. <https://doi.org/10.21608/ejchem.2017.5510> (2017).
25. Neil, B., Deborah, C., Philip, G. H. & Gavin, S. W. Silver modified Degussa P25 for the photocatalytic removal of nitric oxide. *Int. J. Photo Energy* **20**, 8 (2007).
26. Derakhshan, S. J., Karimi, L., Zohoori, S., Davodiroknabadi, A., & Lessani, L.: Antibacterial and self-cleaning properties of cotton fabric treated with TiO₂/Pt (2018).
27. Segal, L. G. J. M. A., Creely, J. J., Martin, A. E. Jr. & Conrad, C. M. An empirical method for estimating the degree of crystallinity of native cellulose using the X-ray diffractometer. *Text. Res. J.* **29**(10), 786–794. <https://doi.org/10.1177/004051755902901003> (1959).
28. S.A.S.: Standards Association of Australia, Standard AS/NZS 43399; Australian/New Zealand Standards, Home bush, Australia (1996).
29. Sharma, D. & Singh, M. Effect of dyeing and finishing treatments on sun protection of woven fabrics: A study. *Colourage* **20**, 69–74 (2001).
30. AATCC (Technical manual of American Association of Textile Chemists and Colorists). 77, 341–343 (2002)
31. AATCC (Technical manual of American association of textile chemistry and colorist method). Test method of antibacterial activity of fabrics, detection of agar plate method 90(52):268–269 (1974).
32. Bozzi, A., Yuranova, T., Guasaquillo, I., Laub, D. & Kiwi, J. Self-cleaning of modified cotton textiles by TiO₂ at low temperatures under daylight irradiation. *J. Photochem. Photobiol. A Chem.* **174**(2), 156–164. <https://doi.org/10.1016/j.jphotochem.2005.03.019> (2005).
33. Ibrahim, N. A., Amr, A., Eid, B. M., Mohamed, Z. E. & Fahmy, H. M. Poly (acrylic acid)/poly (ethylene glycol) adduct for attaining multifunctional cellulosic fabrics. *Carbohydr. Polym.* **89**(2), 648–660. <https://doi.org/10.1016/j.carbpol.2012.03.068> (2012).
34. Hebeish, A., El-Rafie, M. H., El-Sheikh, M. A. & El-Naggar, M. E. Nanostructural features of silver nanoparticles powder synthesized through concurrent formation of the nanosized particles of both starch and silver. *J. Nanotechnol.* <https://doi.org/10.1155/2013/201057> (2013).
35. Yang, X. H. *et al.* Synthesis of silver-titanium dioxide nanocomposites for antimicrobial applications. *J. Nanopart. Res.* **16**, 1–13. <https://doi.org/10.1007/s11051-014-2526-8> (2014).
36. Min, Y. *et al.* Silver@ mesoporous anatase TiO₂ core-shell nanoparticles and their application in photocatalysis and SERS sensing. *Coatings* **12**(1), 64. <https://doi.org/10.3390/coatings12010064> (2022).
37. Cosgrove, T. (ed.) *Colloid Science: Principles, Methods and Applications* (Wiley, 2010).
38. Yang, F. C. *et al.* Preparation and characterization of functional fabrics from bamboo charcoal/silver and titanium dioxide/silver composite powders and evaluation of their antibacterial efficacy. *Mater. Sci. Eng. C* **32**(5), 1062–1067. <https://doi.org/10.1016/j.msec.2009.11.016> (2012).
39. El-Naggar, M. E., Shaarawy, S., Abdel-Aziz, M. S., Abd El Moneim, H. K. & Youssef, A. M. Functionalization of cotton fabrics with titanium oxide doped silver nanoparticles: Antimicrobial and UV protection activities. *Luminescence* **37**(5), 854–864. <https://doi.org/10.1002/bio.4229> (2022).
40. Ali, M. F., Gashti, M. P., Shamei, A. & Kiumarsi, A. Deposition of silver nanoparticles on carbon nanotube by chemical reduction method: Evaluation of surface, thermal and optical properties. *Super Lattices Microstruct.* **52**(1), 50–62. <https://doi.org/10.1016/j.spmi.2012.04.015> (2012).
41. Jafari-Kiyan, A., Karimi, L. & Davodiroknabadi, A. Producing colored cotton fabrics with functional properties by combining silver nanoparticles with nano titanium dioxide. *Cellulose* **24**, 3083–3094. <https://doi.org/10.1007/s10570-017-1308-8> (2017).
42. Xu, Q., Wang, P., Zhang, Y. & Li, C. Durable antibacterial and UV protective properties of cotton fabric coated with carboxymethyl chitosan and Ag/TiO₂ composite nanoparticles. *Fibers Polym.* <https://doi.org/10.1007/s12221-021-0352-z> (2021).
43. Norouzi, M. & Maleknia, L. Photocatalytic effects of nanoparticles of TiO₂ in order to design self-cleaning textiles. *Asian J. Chem.* **22**(8), 5930–5936 (2010).
44. Sami, M. S. & Barakat, O. Use of nanotechnology to achieve the best functional characteristics of the fabrics sheets used in hospitals. *Egypt. J. Chem.* **61**(4), 705–715. <https://doi.org/10.21608/ejchem.2018.2892.1238> (2018).
45. Abou-Okeil, A., Eid, R. A. A. & Amr, A. Multi-functional cotton fabrics using nano-technology and environmentally friendly finishing agents. *Egypt. J. Chem.* <https://doi.org/10.21608/ejchem.2017.5510> (2017).
46. Alvarez-Amparán, M. A. *et al.* Characterization and photocatalytic activity of TiO₂ nanoparticles on cotton fabrics, for antibacterial masks. *Appl. Nanosci.* **12**, 4019–4032. <https://doi.org/10.1007/s13204-022-02634-z> (2022).
47. Ramkumar, V. S. *et al.* Biofabrication and characterization of silver nanoparticles using aqueous extract of seaweed *Enteromorpha compressa* and its biomedical properties. *Biotechnol. Rep.* **14**, 1–7. <https://doi.org/10.1016/j.btre.2017.02.001> (2017).
48. Khorrami, S., Zarrabi, A., Khaleghi, M., Danaei, M. & Mozafari, M. R. Selective cytotoxicity of green synthesized silver nanoparticles against the MCF-7 tumor cell line and their enhanced antioxidant and antimicrobial properties. *Int. J. Nanomed.* <https://doi.org/10.2147/IJN.S189295> (2018).
49. Li, N., Pranantyo, D., Kang, E. T., Wright, D. S. & Luo, H. K. A simple drop-and-dry approach to grass-like multifunctional nano-coating on flexible cotton fabrics using in situ-generated coating solution comprising titanium-oxo clusters and silver nanoparticles. *ACS Appl. Mater. Interfaces* **12**(10), 12093–12100. <https://doi.org/10.1021/acsami.9b22768> (2020).
50. Wang, L. *et al.* Study on properties of modified nano-TiO₂ and its application on antibacterial finishing of textiles. *J. Ind. Text.* **44**(3), 351–372. <https://doi.org/10.1177/1528083713487758> (2014).
51. Akhavan, F. & Montazerb, S. M. In situ sonosynthesis of nano TiO₂ on cotton fabric. *Ultrason. Sonochem.* **21**, 681–691. <https://doi.org/10.1016/j.ultsonch.2013.09.018> (2014).
52. Zille, A. *et al.* Application of nanotechnology in antimicrobial finishing of biomedical textiles. *Mater. Res. Express.* **1**(3), 032003. <https://doi.org/10.1088/2053-1591/1/3/032003> (2014).
53. Perelshtein, I., Apperlot, G., Perkas, N., Grinblat, J. & Gedanken, A. A one-step process for the antimicrobial finishing of textiles with crystalline TiO₂ nanoparticles. *Chem. A Eur. J.* **18**(15), 4575–4582. <https://doi.org/10.1002/chem.201101683> (2012).
54. Mohamed, A. L., El-Naggar, M. E. & Hassabo, A. G. Preparation of hybrid nanoparticles to enhance the electrical conductivity and performance properties of cotton fabrics. *J. Mater. Res. Technol.* **12**, 542–554. <https://doi.org/10.1016/j.jmrt.2021.02.035> (2021).
55. Li, X., Zhu, D. & Wang, X. Evaluation on dispersion behavior of the aqueous copper nano-suspensions. *J. Colloid Interface Sci.* **310**(2), 456–463. <https://doi.org/10.1016/j.jcis.2007.02.067> (2007).
56. Fujishima, A. Titanium dioxide photocatalysis: Present situation and future approaches. *Comptes Rendus Chim.* **9**(5–6), 750–760. <https://doi.org/10.1016/j.crci.2005.02.055> (2006).
57. Ni, M., Leung, M. K. H., Leung, D. Y. C. & Sumathy, K. A review and recent developments in photocatalytic water-splitting using TiO₂ for hydrogen production. *Renew. Sustain. Energy Rev.* **11**, 401–425. <https://doi.org/10.1016/j.rser.2005.01.009> (2007).
58. Pelaez, M. *et al.* A review on the visible light active titanium dioxide photocatalysts for environmental applications. *Appl. Catal. B Environ.* **125**, 331–349. <https://doi.org/10.1016/j.apcatb.2012.05.036> (2012).
59. Diaz-Urbe, C. E. *et al.* Photocatalytic degradation of methylene blue by the Anderson-type polyoxomolybdates/TiO₂ thin films. *Polyhedron* **149**, 163–170. <https://doi.org/10.1016/j.poly.2018.04.027> (2018).
60. MiarAlipour, S., Friedmann, D., Scott, J. & Amal, R. TiO₂/porous adsorbents: Recent advances and novel applications. *J. Hazard. Mater.* **341**, 404–423. <https://doi.org/10.1016/j.jhazmat.2017.07.070> (2018).

61. Nadimi, M., Saravani, A. Z., Aroon, M. A. & Pirbazari, A. E. Photodegradation of methylene blue by a ternary magnetic TiO₂/Fe₃O₄/graphene oxide nanocomposite under visible light. *Mater. Chem. Phys.* **225**, 464–474. <https://doi.org/10.1016/j.matchemphys.2018.11.029> (2019).
62. Nasr, M., Eid, C., Habchi, R., Miele, P. & Bechelany, M. Recent progress on titanium dioxide nanomaterials for photocatalytic applications. *ChemSusChem* **11**(18), 3023–3047. <https://doi.org/10.1002/cssc.201800874> (2018).
63. Harikishore, M., Sandhyarani, M., Venkateswarlu, K., Nellaippan, T. A. & Rameshbabu, N. Effect of Ag doping on antibacterial and photocatalytic activity of nanocrystalline TiO₂. *Proced. Mater. Sci.* **6**, 557–566. <https://doi.org/10.1016/j.mspro.2014.07.071> (2014).
64. Noreen, Z. *et al.* Visible light sensitive Ag/TiO₂/graphene composite as a potential coating material for control of *Campylobacter jejuni*. *Mater. Sci. Eng. C* **98**, 125–133. <https://doi.org/10.1016/j.msec.2018.12.087> (2019).
65. Din, M. I., Khalid, R. & Hussain, Z. Minireview: Silver doped titanium dioxide and silver doped zinc oxide photocatalysts. *Analyt. Lett.* **51**, 2719–2907. <https://doi.org/10.1080/00032719.2017.1363770> (2017).
66. Khan, M. R., Chuan, T. W., Yousuf, A., Chowdhury, M. N. K. & Cheng, C. K. Schottky barrier and surface plasmonic resonance phenomena towards the photocatalytic reaction: Study of their mechanisms to enhance photocatalytic activity. *Catal. Sci. Technol.* **5**(5), 2522–2531. <https://doi.org/10.1039/x0xx00000x> (2015).
67. Furube, A. & Hashimoto, S. Insight into plasmonic hot-electron transfer and plasmon molecular drive: New dimensions in energy conversion and nanofabrication. *NPG Asia Mater.* **9**, e454–e424. <https://doi.org/10.1038/am.2017.191> (2017).

Acknowledgements

Prof. Dr. Mai SA Hussien, Nanoscience Laboratory for Environmental and Biomedical Applications (NLEBA), Nuclear Lab., Department of Physics, Faculty of Education, Ain Shams University, Egypt, for kind assistant in nanoparticles synthesis.

Author contributions

Conceptualization, M.A., E.A., and A.A.; visualization, M.A., E.A. and A.A.; investigation, M.A., E.A., A.A., and S.E.; methodology, M.A., E.A., A.A. and S.E.; resources, M.A., A.A., A.A. and S.E.; data curation, M.A., E.A., A.A. and S.E.; writing original draft preparation, M.A., E.A., A.A. S.E. and; formal analysis, M.A., E.A., A.A. and S.E.; writing, review and editing, M.A. and S.E.; supervision, E.A., A.A. and M.A. All authors have read and agreed to the published version of the manuscript.

Funding

Open access funding provided by The Science, Technology & Innovation Funding Authority (STDF) in cooperation with The Egyptian Knowledge Bank (EKB).

Competing interests

The authors declare no competing interests.

Additional information

Correspondence and requests for materials should be addressed to M.A.-S.A.

Reprints and permissions information is available at www.nature.com/reprints.

Publisher's note Springer Nature remains neutral with regard to jurisdictional claims in published maps and institutional affiliations.



Open Access This article is licensed under a Creative Commons Attribution 4.0 International License, which permits use, sharing, adaptation, distribution and reproduction in any medium or format, as long as you give appropriate credit to the original author(s) and the source, provide a link to the Creative Commons licence, and indicate if changes were made. The images or other third party material in this article are included in the article's Creative Commons licence, unless indicated otherwise in a credit line to the material. If material is not included in the article's Creative Commons licence and your intended use is not permitted by statutory regulation or exceeds the permitted use, you will need to obtain permission directly from the copyright holder. To view a copy of this licence, visit <http://creativecommons.org/licenses/by/4.0/>.

© The Author(s) 2024